## PAPER

Check for updates

# Energy-saving electrolytic γ-MnO₂ generation: non-noble metal electrocatalyst gas diffusion electrode as cathode in acid solution

Jing Tang, [iD] *[a] Hui Min Meng[b] and Mei Yang Ji[b]

γ-MnO₂, which is commercially used as an electrode material in batteries, is produced using large amounts of energy and leads to the production of high pollution as a secondary product. Ideally, this material should be fabricated by energy efficient, non-polluting methods at a reasonable cost. This study reports the green fabrication of γ-MnO₂ into a gas diffusion electrode with Pt-free catalysts in acid solution. Cobalt oxide nanoparticles were deposited on few-layer graphene sheets produced *via* a simple sintering and ultrasonic mixing method, leading to the fabrication of cobalt oxide/few-layer graphene. $Co_3O_4$ nanoparticles are irregularly shaped and uniformly distributed on the surface of the few-layer graphene sheets. Characterization was conducted by X-ray diffraction, X-ray photoelectron spectroscopy, and field emission scanning electron microscopy. Electrochemical characterization revealed the performance of cobalt oxide/few-layer graphene gas diffusion electrode in an electrolyte of 120 g $L^{-1}$ manganese sulfate + 30 g $L^{-1}$ sulfuric acid at 100 A $m^{-2}$ at 80 °C. The cobalt oxide/few-layer graphene gas diffusion electrode exhibited a lower cell voltage of 0.9 V and higher electric energy savings of approximately 50% compared with traditional cathodes (copper and carbon).

## Introduction

Electrolytic manganese dioxide (EMD) may be potentially inexpensive, relatively energy dense, safe, water compatible, and non-toxic when used as an electrode material.[1] However, the deposition of EMD, particularly at an industrial scale, not only consumes excessive electric energy but also causes environmental damage because of the acid fog generated by the electrolytic cell.[2] Factories have ceased producing EMDs to protect the environment. To overcome this problem, optimization methods have been proposed to reduce the energy required for electrodeposition of manganese dioxide ($MnO_2$). Biswal[3] *et al.* investigated the energy consumption of $MnO_2$ electrodeposition with the introduction of F127 (25F) in the bath and found that energy consumption can be decreased by up to 11%. In our previous work, a platinum (Pt) catalyst gas diffusion electrode (GDE) used as a cathode for electrodeposition of $MnO_2$ is proposed to save energy by approximately 60% and protect the environment.[4] In theory, when a Pt catalyst GDE is applied, the oxygen reduction reaction (ORR) replaces the hydrogen evolution reaction (HER). Pt and its alloys are the best-known ORR catalysts[5] in acid. However, catalyst-based metal-free materials,

such as Pt, are not widely applied[6] due to their high cost and low abundance. Although the field of electrode manufacturing has progressed considerably, the development of oxygen electrode catalysts with high activity at low cost in acid remains challenging.[7]

Herein, a metal-free catalyst GDE with cobalt oxide nanoparticles on few-layer graphene (FLG) is proposed as a cathode to save electrical energy (50%) and achieve environment-friendly electrodeposition to meet production requirements. The proposed catalyst and method surprisingly exhibited high performance in acid solution. The manufacturing method of the $Co_3O_4$/FLG GDE is simple and inexpensive; it may potentially replace the commercial Pt/C GDE in electrodeposition of $MnO_2$.

## Experiment

A general two-step method was used to synthesize the $Co_3O_4$/FLG catalyst. First, 2.5 g of cotton was sintered with 5 g of cobalt nitrate solution to produce $Co_3O_4$ nanoparticles, after which calcination was performed at 400 °C for 2 h[8] and then it was milled for 3 h. Then, 0.2 g of $Co_3O_4$ nanoparticles was dispersed in 20 mL of ethanol by sonication. Subsequently, few layer graphene wrapped in a microporous membrane (450 μm) was dipped and sonicated in the $Co_3O_4$ solution for 8 h and centrifuged to form the $Co_3O_4$/FLG hybrid (Fig. 1). The sample was freeze-dried overnight at 60 °C. The GDE is a three-layer structure which consists of diffusive layer, substrate and

*[a]School of Mechanical Engineering, Liaoning Shihua University, Fushun 113001, China. E-mail: fstangcandy@126.com*

*[b]Corrosion and Protection Center, Institute for Advance Materials and Technology, University of Science and Technology Beijing, No. 30, Xueyuan Road, Haidian District, Beijing 100083, China. Tel: +86 024 56860273*
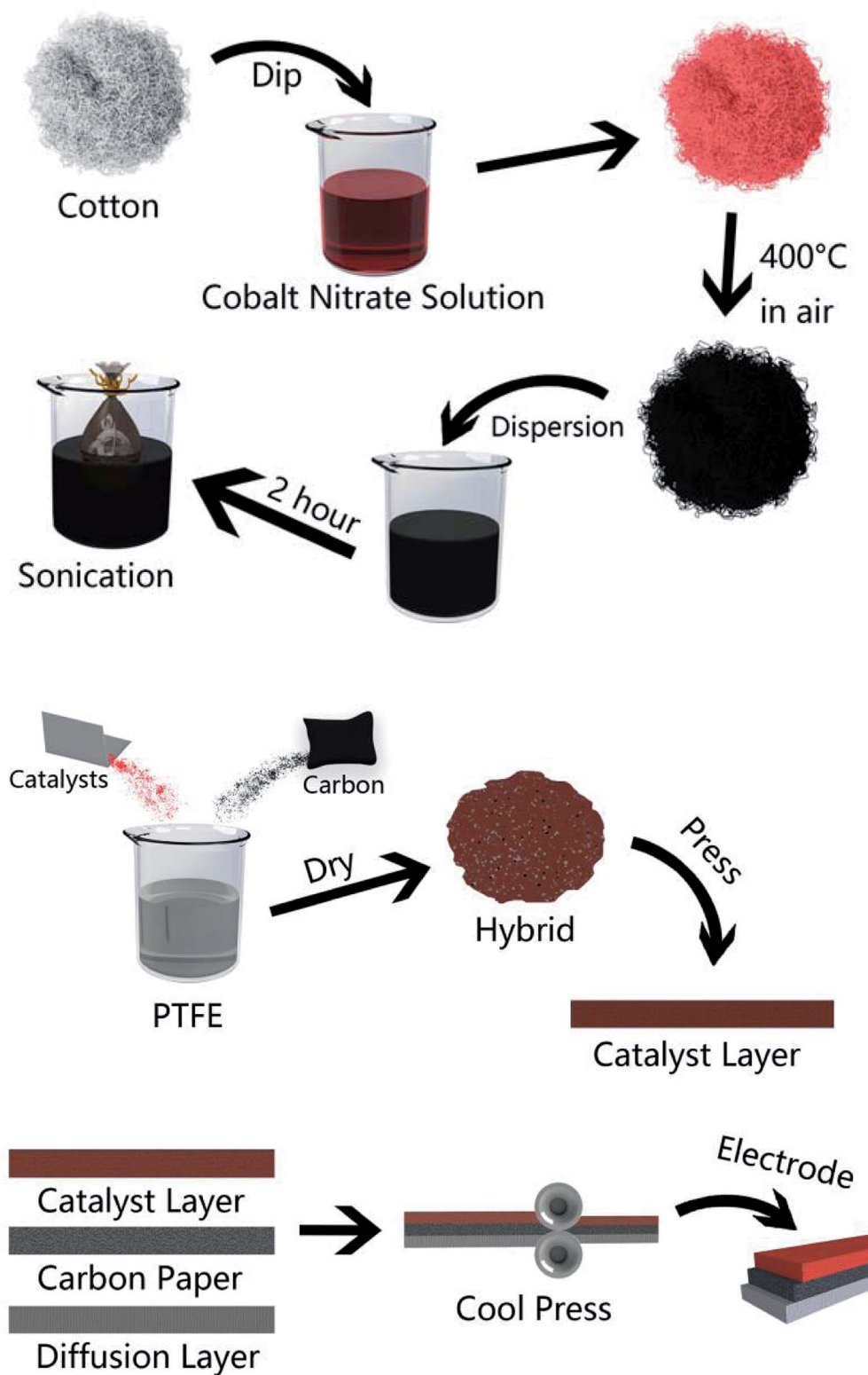
Fig. 1 Schematic of the methods used to prepare the $Co_3O_4$/FLG nanocatalyst and $Co_3O_4$/FLG GDE.

catalyst layer. Before the experiment began, the 60% PTFE was painted onto carbon paper (Phychemi Company Limited, China), and then it was sintered at 350 °C for 30 min. 0.25 g of acetylene black, 0.3 g of $Na_2SO_4$, 0.25 g of activated carbon powder, 0.17 g of 60% PTFE (Hesen, Shanghai, China), and 100 mL of ethanol was mixed and then stirred at 80 °C to wet paste. The wet paste was cool pressed to prepare the diffusion layer (0.4 mm). The catalyst layer was prepared by blending non-

noble metal electrocatalysts, carbon black, activated carbon powder, 60% PTFE and 100 mL of ethanol as a dispersant and the rolling process was same as the diffusion layer. Furthermore, the diffusion layer and the catalyst layer was rolled on two sides of the carbon paper to obtain about 0.8 mm flat sheet. The structures and crystal phases of the catalyst were analyzed by X-ray diffraction (XRD Ultima VI) with Cu K$_\alpha$ radiation ($\lambda$ = 0.15406 nm) operating at 40 kV and 40 mA. The microstructures of the catalyst and GDE were investigated using a transmission electron microscope (TEM, JEOL JEM-2100F). Surface characterization of the samples was conducted by X-ray photoelectron spectroscopy (XPS, AxIS-ULTRA-DLD) with a Mg K$_\alpha$ anode. Binding energies were calibrated based on the C 1s peak (284.8 eV).[9] Electrochemical tests were performed using a potentiostat. Here, the working electrodes were GDEs, and a Ti–Mn array was used as the counter electrode at 100 A m$^{-2}$. The electrolyte was 120 g dm$^{-3}$ + 30 g dm$^{-3}$ at 80 °C (Fig. 2).

## Results and discussion

XRD was applied to determine the phase identity and structural information of the samples. Fig. 3 shows the XRD patterns of $Co_3O_4$ and $Co_3O_4$/FLG. The characteristic peaks of (111), (220), (311), (222), (400), (422), (511), and (440) are in agreement with those of the standard patterns of $Co_3O_4$ with a face-centered cubic structure,[10] thereby suggesting that $Co(NO_3)_2 \cdot 6H_2O$ was transformed into $Co_3O_4$ at 400 °C. The relatively sharp diffraction peak at $2\theta = 24.5°-27.5°$ in the XRD pattern can be indexed as the graphite layer (200), indicating that the graphene is not single layer. This result is same as the research of Junming Xu.[11] The $Co_3O_4$ in $Co_3O_4$/FLG is relatively weaker than pure $Co_3O_4$, possibly resulting in more disordered stacking and less agglomeration on the graphene sheets in the composite.[12] Graphene sheets present the advantages of a highly exposed surface area and electrical conductivity, which contribute to the improved electrochemical performance of $Co_3O_4$.

TEM was performed to confirm the structure of the $Co_3O_4$/FLG. The TEM images in Fig. 4 shows several large $Co_3O_4$
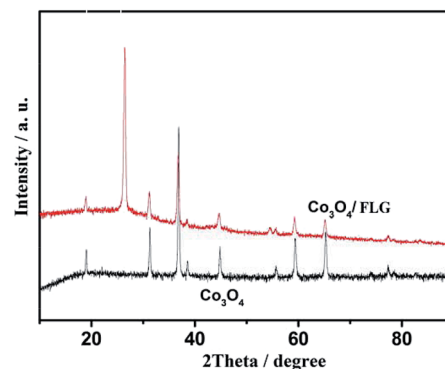
Fig. 3   Characterization of $Co_3O_4$/FLG and $Co_3O_4$ catalysts.

nanoparticles formed on the graphene sheets, thus suggesting that $Co_3O_4$ nanoparticles were doped onto the graphene sheets by the dipping method. Even after considerable sonication
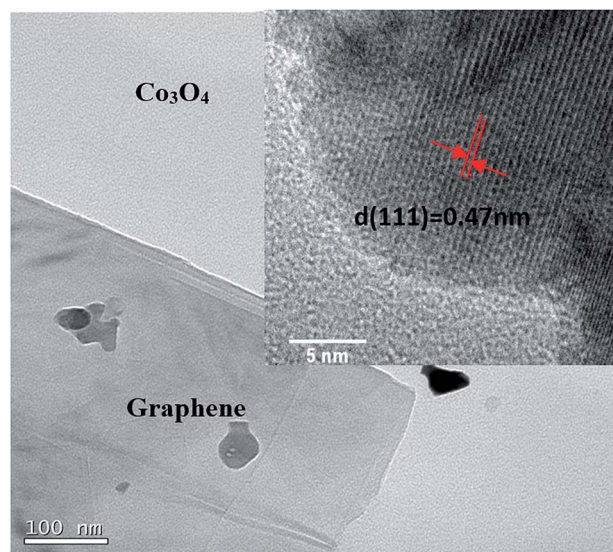
Fig. 4   High Resolution Transmission Electron Microscope (HRTEM) images of the $Co_3O_4$/FLG and $Co_3O_4$ inside.
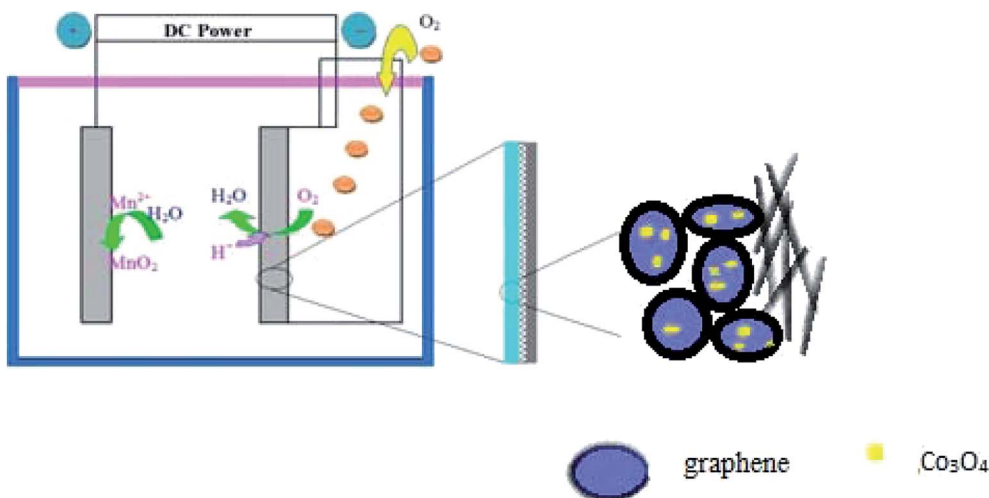
Fig. 2   Schematic of $Co_3O_4$/FLG GDE electrolysis.

during the preparation of the TEM specimen, $Co_3O_4$ nanoparticles were still closely distributed on the graphene surface. $Co_3O_4$ nanoparticles are irregularly shaped and uniformly distributed on the surface of the graphene sheets. The interplanar distance with a spacing of 0.47 nm is consistent with the (111) facet of $Co_3O_4$.[13]

The XPS spectra reveal the elemental information of the $Co_3O_4$/FLG catalyst. From the survey scan of the $Co_3O_4$/FLG (Fig. 5a), Co, C, and O are the three elements that make up $Co_3O_4$/FLG. This result demonstrates that Co was successfully doped into the graphene sheets *via* the proposed two-step process. The peak at 284.4 eV (Fig. 5b) is assigned to the characteristic peaks of C 1s.[14] Peaks at 284.4, 285.3, and 288.9 eV are attributed to $sp^2$ graphitic carbon (C=C) bonds, carbon bonds with $sp^3$ hybridization, and O–C–O bonds, respectively.[15] The peaks located at 780.62 and 795.93 eV (Fig. 5c) are assigned to the binding energies of Co $2p_{3/2}$ and Co $2p_{1/2}$, respectively, with two prominent shake-up satellite peaks at 786.5 and 804.1 eV, both of which confirm that $Co_3O_4$ was obtained.[16] The predominant O 1s peak (Fig. 5d) at 530.1 and 532.5 eV corresponds to that of O species in the spinel $Co_3O_4$ phase and the hydroxyl groups adsorbed on the surface due to our *ex situ* experimental conditions, respectively.[17] Therefore, $Co_3O_4$/FLG is likely composed of $Co_3O_4$ on the graphene sheets surface.

Fig. 6 shows the cell voltage of traditional electrode, C GDE and $Co_3O_4$/FLG GDE at 100 A m$^{-2}$ in 30 g dm$^{-3}$ $H_2SO_4$ + 120 g

$dm^{-3}$ $MnSO_4$ at 80 °C. All the average anode potential of the experiments is almost the same which is about 0.62 V *vs.* $Hg_2SO_4$ at 100 A m$^{-2}$ and the electrodeposition efficiency of γ-$MnO_2$ is not affected. However, the cell voltage of the electrodeposition of $MnO_2$ using $Co_3O_4$/FLG GDE as cathode is lower than that of the electrodeposition of $MnO_2$ using traditional electrode. It is because the anode reaction of traditional electrode is the same as that of gas diffusion electrode. The gas diffusion electrode is
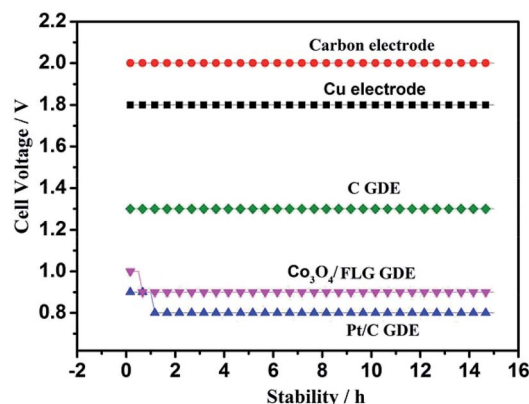


Fig. 6 Cell voltage of traditional electrode, carbon electrode, Cu electrode, C GDE, $Co_3O_4$/FLG GDE and Pt/C GDE at 100 A m$^{-2}$ in 30 g dm$^{-3}$ $H_2SO_4$ + 120 g dm$^{-3}$ $MnSO_4$ at 80 °C.
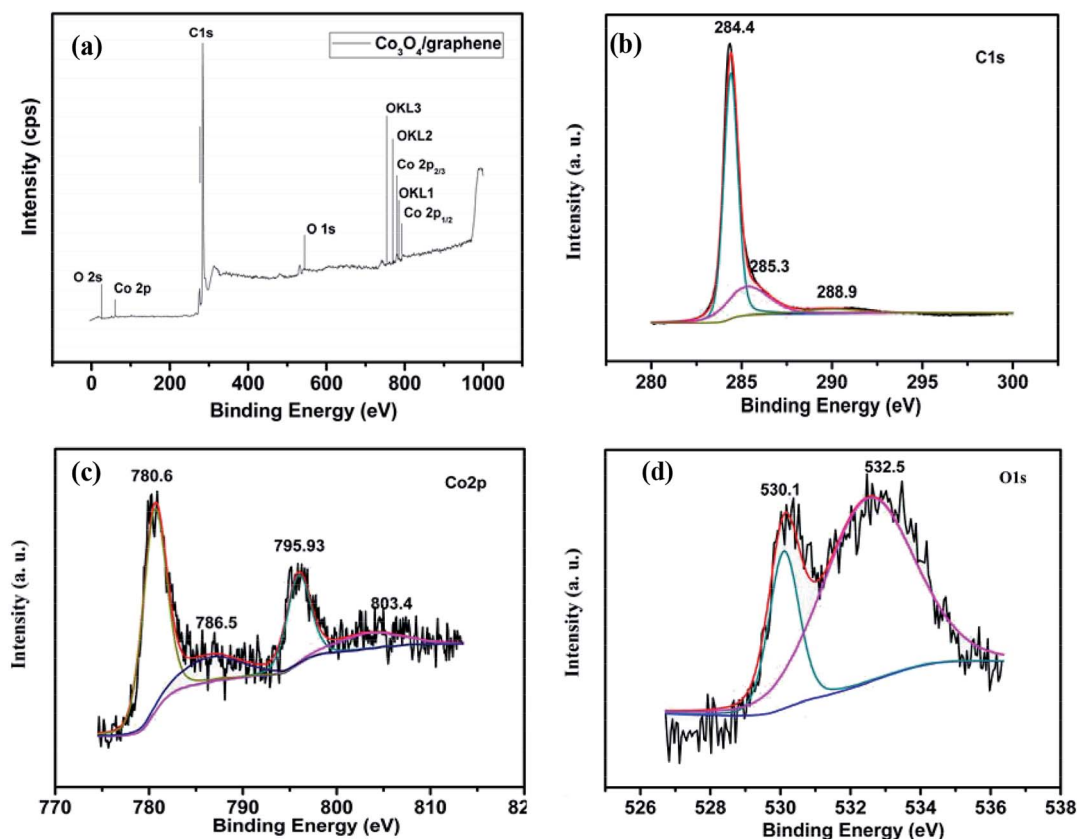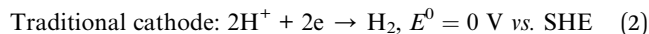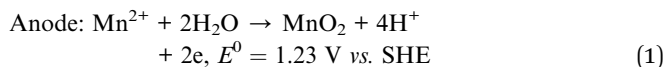


Fig. 5 XPS spectra of (a) the $Co_3O_4$/FLG, (b) C 1s spectra of the $Co_3O_4$/FLG, (c) Co 2p spectra of the $Co_3O_4$/FLG and (d) O 1s spectra of the $Co_3O_4$/FLG.
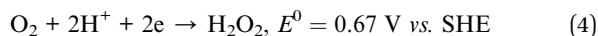
employed in the electrolytic manganese dioxide cell instead of the traditional electrode, the electrochemical reaction is:

$$\text{Anode: } Mn^{2+} + 2H_2O \rightarrow MnO_2 + 4H^+ + 2e, \ E^0 = 1.23 \text{ V } vs. \text{ SHE} \tag{1}$$

$$\text{Traditional cathode: } 2H^+ + 2e \rightarrow H_2, \ E^0 = 0 \text{ V } vs. \text{ SHE} \tag{2}$$

Gas diffusion electrode as cathode: overall 4 electron reaction forming water

$$O_2 + 4H^+ + 4e \rightarrow 2H_2O, \ E^0 = 1.229 \text{ V } vs. \text{ SHE} \tag{3}$$
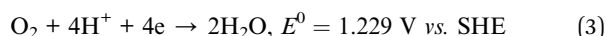
Or two electron process, forming unwanted $H_2O_2$

$$O_2 + 2H^+ + 2e \rightarrow H_2O_2, \ E^0 = 0.67 \text{ V } vs. \text{ SHE} \tag{4}$$

After doping of the $Co_3O_4$ nanoparticles into the graphene sheets, the cell voltage of the $Co_3O_4$/FLG GDE decreased drastically to 0.9 V, similar to the ORR catalyzed by a high-quality commercial Pt/C GDE (0.8 V). The Pt/C catalyst is acknowledged to be the most effective catalyst for oxygen reduction reaction in acid media. In our previous studies, the ORR, catalysed by the Pt/C catalyst, proceeds *via* both the two electron transfer and the four-electron transfer, but four-electron transfer is the main process in 30 g dm$^{-3}$ $H_2SO_4$ + 120 g dm$^{-3}$ $MnSO_4$ at 80 °C.[18] However, cell voltage of C GDE in $H_2SO_4$ is 0.5 V higher than the Pt/C GDE, as expected, since C GDE features a two electrons transfer to product $H_2O_2$ in acid solution which is same as the research of Ichiro Yamanaka.[19] The cell voltage of C GDE is 1.3 V which is 0.4 V higher than that of $Co_3O_4$/graphene GDE in electrodeposition of $\gamma$-$MnO_2$ while it was similar to Pt/C GDE, indicating that ORR of $Co_3O_4$/FLG GDE in 30 g dm$^{-3}$ $H_2SO_4$ + 120 g dm$^{-3}$ $MnSO_4$ at 80 °C is both two electrons transfer (eqn (4)) with the formation of $H_2O_2$ and the four-electron transfer (eqn (3)) producing $H_2O$.[20]

In order to manifest the cause of the high activity of the $Co_3O_4$/FLG GDE in the electrodeposition of $MnO_2$, a two-electrode cell assembly was fabricated using the proposed GDE as the cathode, a Ti-based Ti–Mn array as the anode, and 120 g L$^{-1}$ $MnSO_4$ + 30 g L$^{-1}$ $H_2SO_4$ as the electrolyte. Fig. 7 shows the cell voltage–time curves of $Co_3O_4$ GDE, FLG GDE, $Co_3O_4$/FLG GDE, $Co_3O_4$/C GDE, $MnO_2$/FLG, Pt/C GDE, carbon electrode, and copper electrode at 100 A m$^{-2}$. $Co_3O_4$ exhibited very poor ORR activity with an initial cell voltage of 1.3 V that increased slowly to 1.6 V after 10 h due to its poor conductivity and the small surface area of $Co_3O_4$.[21] However, The $Co_3O_4$/C GDE revealed poor ORR like $Co_3O_4$ GDE indicating that C didn't make $Co_3O_4$/C GDE work better. The cell voltage of FLG GDE and $MnO_2$/FLG GDE revealed poor ORR activity with a cell voltage of 1.3 V because of low corrosion resistance of the $MnO_2$ and low ORR activity of graphene. However, the $Co_3O_4$/FLG nanocatalyst is much more active than either pure $Co_3O_4$ or FLG nanocatalysts in the electrodeposition of $MnO_2$. The $Co_3O_4$/FLG GDE can save up to $\sim$50% of the electric energy required by traditional cathodes (Cu and C) in Fig. 6. The increased activity of the proposed GDE may be attributed to synergistic effects
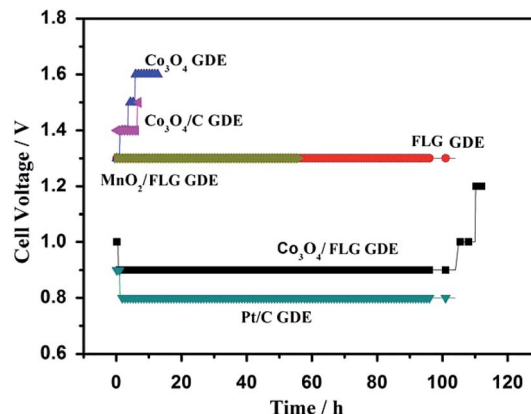


Fig. 7 Cell voltage test: $Co_3O_4$ GDE, FLG GDE, $Co_3O_4$/FLG GDE, $Co_3O_4$/C GDE, $MnO_2$/FLG, Pt/C GDE at 100 A m$^{-2}$ in 30 g dm$^{-3}$ $H_2SO_4$ + 120 g dm$^{-3}$ $MnSO_4$ at 80 °C (all the anode potential of the experiment is almost the same which is about 0.62 V vs. $Hg_2SO_4$).
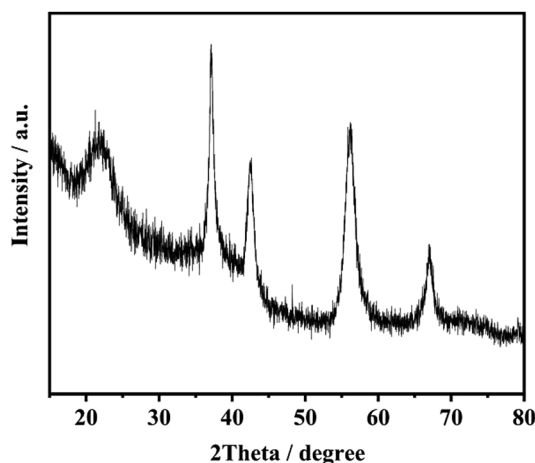


Fig. 8 The product of electrolysis using $Co_3O_4$/FLG GDE.

between the $Co_3O_4$ nanoparticles and FLG[22] with the large electrochemically active surface area[23] and excellent conductivity,[24] which can improve the conductivity and change the charge transfer across the interface. Therefore, $Co_3O_4$ doping of FLG plays a key role in improving the electrocatalytic activity of GDEs for green electrodeposition of $MnO_2$ in acid solution.

Fig. 8 exhibits XRD patterns of the product of electrolysis. The four sharper peaks appeared at 37.3°, 42.7°, 56.5° and 67.3° which are ascribed to the (021), (121), (221) and (061) planes of $\gamma$-$MnO_2$.[25,26]

## Conclusion

In summary, a nanocomposite of $Co_3O_4$/FLG was synthesized through a pyrolysis and dipping process. The nanocomposite is simple and easily obtained in the industry. $Co_3O_4$/FLG was used as a nanocatalyst to catalyze the ORR in the electrodeposition of $MnO_2$. The proposed $Co_3O_4$/FLG nanocomposite GDE exhibited a high activity of 0.9 V at a current density of 100 A m$^{-2}$, 50%

energy savings, and an approximately one fold enhancement compared with those of pure $Co_3O_4$ and FLG electrodes, $Co_3O_4/C$ GDE, and $MnO_2/FLG$ GDE. The $Co_3O_4/FLG$ nanocomposite GDE also displayed better durability in an acid solution (100 h at 100 A m$^{-2}$ in 120 g L$^{-1}$ $MnSO_4$ + 30 g L$^{-1}$ $H_2SO_4$) than the Pt-free GDE.

## Conflicts of interest

There are no conflicts to declare.

## Acknowledgements

## References

1 N. D. Ingale, J. W. Gallaway, M. Nyce, A. Couzis and S. Banerjee, *J. Power Sources*, 2015, **276**, 7–18.

2 S. R. W. Alwi, Z. A. Manan, J. J. Klemeš and D. Huisingh, *J. Cleaner Prod.*, 2014, **71**, 1–10.

3 A. Biswal, M. Minakshi and B. C. Tripathy, *Dalton Trans.*, 2016, **45**, 5557–5567.

4 J. Tang, H. M. Meng and X. Liang, *J. Cleaner Prod.*, 2016, **137**, 903–909.

5 I. E. L. Stephens, A. S. Bondarenko, U. Grønbjerg, J. Rossmeisl and I. Chorkendorff, *Energy Environ. Sci.*, 2012, **5**, 6744–6762.

6 D. S. Geng, Y. Chen, Y. G. Chen, Y. L. Li, R. Y. Li, X. L. Sun, X. Y. Ye and S. Knights, *Energy Environ. Sci.*, 2011, **4**, 760–764.

7 S. Y. Gao, H. Y. Liu and K. Geng, *Nano Energy*, 2015, **12**, 785–793.

8 H. Y. Xu, L. B. Gao, Q. Zhang, J. Y. Li, J. T. Diwu, X. J. Chou, J. Tang and C. J. Xue, *J. Nanomater.*, 2014, **2014**, 1–9.

9 J. G. Yu, G. P. Dai and B. B. Huang, *J. Phys. Chem. C*, 2009, **113**, 16394–16401.

10 K. Wang, R. F. Wang, H. Li, H. Wang, X. F. Mao, V. Linkov and S. Ji, *Int. J. Hydrogen Energy*, 2015, **40**, 3875–3882.

11 J. M. Xu, J. S. Wu, L. L. Luo, X. Q. Chen, H. B. Qin, V. Dravid, S. B. Mi and C. L. Jia, *J. Power Sources*, 2015, **274**, 816–822.

12 Z. S. Wu, W. C. Ren, L. Wen, L. Gao, J. P. Zhao, Z. P. Chen, G. M. Zhou, F. Li and H. M. Cheng, *ACS Nano*, 2010, **4**, 3187–3194.

13 J. J. Zhang, H. H. Wang, T. J. Zhao, K. X. Zhang, X. Wei, Z. D. Jiang, S. Hirano, X. H. Li and J. S. Chen, *ChemSusChem*, 2017, **10**, 2875–2879.

14 B. J. Li, H. Q. Cao, J. Shao, G. Q. Li, M. Z. Qu and G. Yin, *Inorg. Chem.*, 2011, **50**, 1628–1632.

15 A. Siokou, F. Ravani, S. Karakalos, O. Frank, M. Kalbac and C. Galiotis, *Appl. Surf. Sci.*, 2011, **257**, 9785–9790.

16 H. Xia, D. D. Zhu, Z. T. Luo, Y. Yu, X. Q. Shi, G. L. Yuan and J. P. Xie, *Sci. Rep.*, 2013, **3**, 2978.

17 B. B. Varghese, T. C. Hoong, Z. Y. Wu, M. V. Reddy, B. V. Chowdari, A. T. S. Wee, V. B. C. Tan, C. T. Lim and C. H. Sow, *Adv. Funct. Mater.*, 2007, **17**, 1932–1939.

18 J. Tang, H. M. Meng, S. Li, M. H. Yu, H. Li and J. H. Shi, *Electrochim. Acta*, 2015, **170**, 92–97.

19 I. Yamanaka, T. Hashimoto, R. Ichihashi and K. Otsuka, *Electrochim. Acta*, 2008, **53**, 4824–4832.

20 K. Wang, R. F. Wang, H. Li, H. Wang, X. F. Mao, V. Linkov and S. Ji, *Int. J. Hydrogen Energy*, 2015, **40**, 3875–3882.

21 L. Wang, D. L. Wang, J. S. Zhu and X. Liang, *Ionics*, 2013, **19**, 215–220.

22 Y. Y. Liang, Y. G. Li, H. L. Wang, J. G. Zhou, J. Wang, T. Regier and H. J. Dai, *Nat. Mater.*, 2011, **10**, 780–786.

23 Q. Liu, J. T. Jin and J. Y. Zhang, *ACS Appl. Mater. Interfaces*, 2013, **5**, 5002–5008.

24 C. X. Wang, P. H. Shi, X. D. Cai, Q. J. Xu, X. J. Zhou, X. L. Zhou, D. Yang, J. C. Fan, Y. L. Min, H. H. Ge and W. F. Yao, *J. Phys. Chem. C*, 2016, **120**, 336–344.

25 J. Zhao, Z. Tao, J. Liang and J. Chen, *Cryst. Growth Des.*, 2008, **8**, 2799–2805.

26 J. Tang, H. M. Meng and L. L. Huang, *RSC Adv.*, 2014, **4**, 16512–16516.